Photochemical & Photobiological Sciences (2024) 23:803–814
https://doi.org/10.1007/s43630-024-00544-3

COMMUNICATIONS

Fabrication and characterization of microporous soft templated photoactive 3D materials for water disinfection in batch and continuous flow

Miriana Vadala[1] · Doru C. Lupascu[1] · Anzhela Galstyan[2]

Received: 24 October 2023 / Accepted: 1 February 2024 / Published online: 11 March 2024

Abstract
Water cleaning can be provided in batch mode or in continuous flow. For the latter, some kind of framework must withhold the cleaning agents from washout. Porous structures provide an ideal ratio of surface to volume for optimal access of the water to active sites and are able to facilitate rapid and efficient fluid transport to maintain a constant flow. When functionalized with suitable photoactive agents, they could be used in solar photocatalytic disinfection. In this study, we have used the sugar cube method to fabricate PDMS-based materials that contain three different classes of photosensitizers that differ in absorption wavelength and intensity, charge as well as in ability to generate singlet oxygen. The obtained sponges are characterized by scanning electron microscopy and digital microscopy. Archimede's method was used to measure porosity and density. We show that the materials can absorb visible light and generate Reactive Oxygen Species (ROS) that are required to kill bacteria. The disinfection ability was tested by examining how irradiation time and operation mode (batch vs. flow) contribute to the performance of the material. The current strategy is highly adaptable to other (medium) pressure-driven flow systems and holds promising potential for various applications, including continuous flow photoreactions.

✉ Anzhela Galstyan
anzhela.galstyan@uni-due.de

[1] Institute for Materials Science and Center for Nanointegration Duisburg-Essen (CENIDE), University of Duisburg-Essen, Universitätsstrasse 15, 45141 Essen, Germany

[2] Faculty of Chemistry, Center for Nanointegration Duisburg-Essen (CENIDE), Centre for Water and Environmental Research (ZWU) and Center of Medical Biotechnology (ZMB), University of Duisburg-Essen, Universitätsstrasse 5, 45141 Essen, Germany

Graphical Abstract

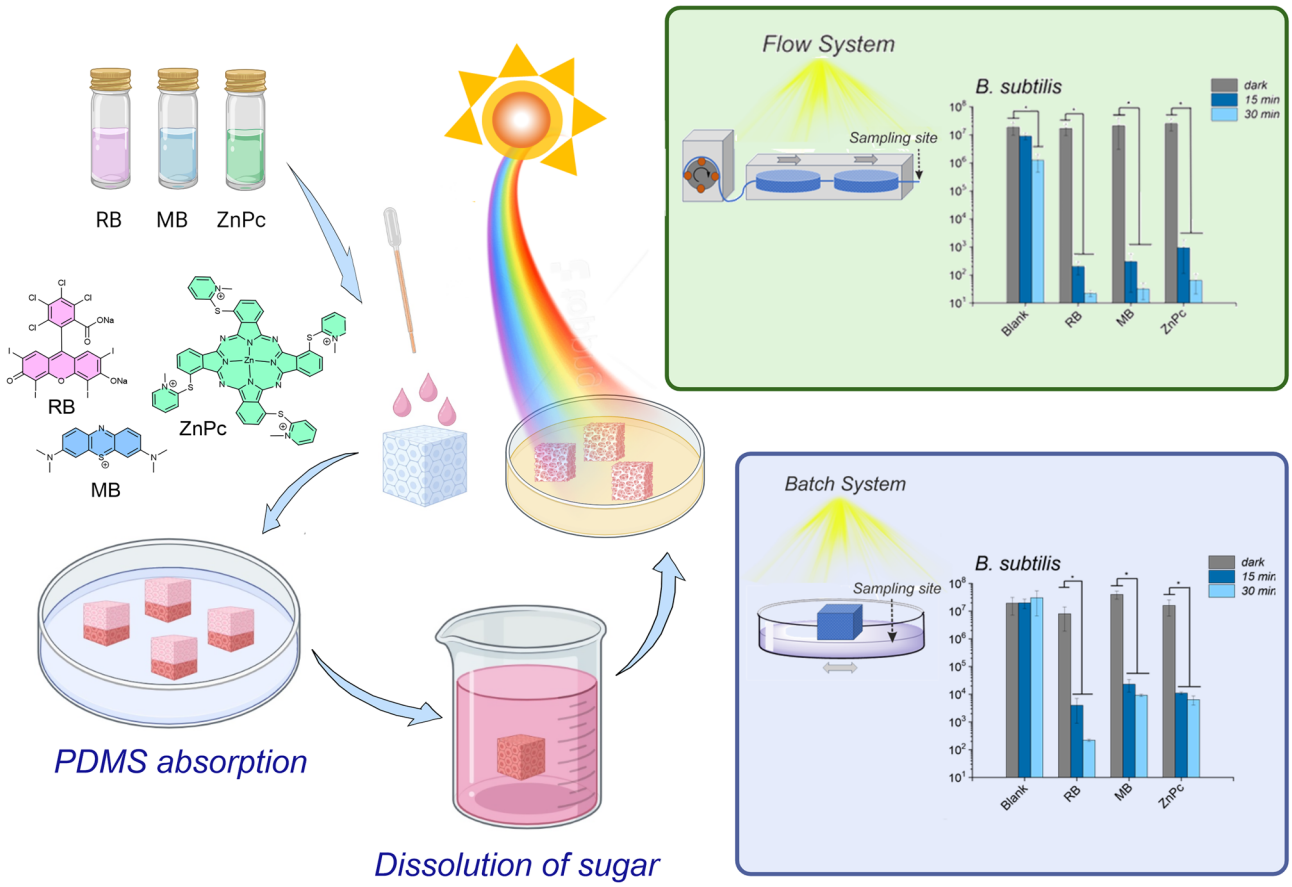

Keywords Photodynamic inactivation · Reactive oxygen species · Bacteria · Continuous flow · Water disinfection

1 Introduction

One of the significant health challenges faced by society is the rising incidence of pathogenic microorganisms that have developed resistance to multiple drugs [1]. In 2019, WHO named antimicrobial resistance (AMR) one of the top 10 global public health threats. Resistant pathogens are considered an "urgent threat" to occur in humans, animals, and the environment emphasizing the importance of a One Health approach to mitigate antimicrobial resistance [2, 3]. One of the essential resources of life, namely water, is both a reservoir and a transmission route for antibiotic-resistant bacteria and resistance genes [4]. These microbes can enter water bodies through various sources, such as sewage and agricultural runoff, which may contain high concentrations of resistant bacteria both from human and animal waste. Therefore, water disinfection plays an important role in combating the spread of AMR, so the demand for sustainable water purification technologies has become a major concern as the world's population grows rapidly, especially in urban areas. Due to concerns regarding the formation of harmful disinfection byproducts by conventional chemical disinfectants, there is a demand for innovative technologies that can effectively disinfect and control microbial growth [5]. In recent years, advancements in materials science have allowed for the development of new materials with improved properties for water treatment processes. For example, the use of nanotechnology has led to the creation of membranes that can filter out even smaller particles and contaminants from water, ensuring a safer supply [6, 7]. Modular water treatment technologies have also emerged as a solution to the challenges faced in providing clean water to urban areas [8, 9]. They allow for water treatment plants to be built and expanded in a more flexible and scalable manner making it easier to meet the increasing demands of growing populations. Energy-efficient processes such as advanced oxidation and renewable energy-powered treatment systems have emerged to minimize the energy and environmental

footprints of cities [10–13]. Solving the issue of antibiotic resistance in water sources demands a comprehensive strategy involving multiple aspects. An important issue is to prioritize the development of new treatment technologies that combat infections without promoting resistance [14, 15]. As a promising alternative to the currently available methods, photodynamic inactivation (PDI) or antimicrobial photodynamic therapy (aPDT) have attracted increasing interest [16–19]. This approach relies on the principle of utilizing visible or near-infrared light to activate photosensitizers (PS). When activated, these PS generate reactive oxygen species (ROS), which have the ability to effectively eliminate a wide range of microorganisms without inducing resistance [20]. The combination of sunlight and a reusable photocatalytic material capable of generating ROS from molecular oxygen is a very promising concept for the development of sustainable systems for the disinfection and decontamination of natural or industrial waters [21, 22]. The use of a flexible and compressible 3D material that has a network of microscopic pores in its structure has the following advantages: (1) high surface-to-volume ratio that favors easy interaction with microorganisms to promote disinfection, (2) porosity that allows high oxygen permeability, and (3) good mechanical stability. The distinct attributes of microporous polymers have been shown to be beneficial not only in water purification but also in other areas including gas separation and storage, catalysis, 3D cell culture, sensing, and drug delivery [23–26]. To obtain photoactive porous materials, the implementation of molecular PS in bulk material is necessary. Generally, the immobilization of photocatalysts enhances their stability, recycling capability, and ease of separation from the reaction mixture [27–29]. This enables better control and optimization of the photocatalytic process, thereby making it more suitable for large-scale applications, including flow systems [30, 31]. Despite its significant potential in advancing sustainable processing, flow photochemistry faces some hurdles that must be overcome [32]. One of these hurdles is the reduced activity of the systems with fixed catalysis in comparison with suspended catalysts.

Among different carrier polymers polydimethylsiloxane (PDMS), which is a silicone-based polymer, is widely used in various industries and applications [33]. It is known for its high thermal stability, low surface energy, excellent electrical insulation, and biocompatibility. PDMS is highly flexible, transparent, and has a rubbery consistency, making it suitable for applications in harsh environments. Regarding PS, numerous classes are available for use in photodisinfection, and many of them have shown highly encouraging outcomes [17, 18]. The selection of a PS in aPDT is determined by the particular application. In the pursuit of creating sustainable photocatalytic processes, one desired trait is for the PS to preferentially absorb wavelengths in the solar irradiation spectrum. Organic PSs belonging to the phenothiazine, xanthene, or porphyrin groups [34], as well as transition metal complexes, especially Ru(II) complexes, have been widely used in recent years [35].

In this study we have used the sugar leaching method to fabricate PDMS sponges that contain three different types of organic photosensitizers—Rose Bengal (RB—dianionic, commercial), Methylene Blue (MB—monocationic, commercial) and substituted Zn(II)phthalocyanine (ZnPc—tetracationic, synthesized according to our previously published work [36]). These PSs belong to three large and widely used PS families, which have previously been suggested as effective PSs for the photodynamic inactivation of microorganisms (Fig. 1a). They were selected not only based on their exceptional individual aPDT capabilities, but also their capacity to effectively absorb a wide range of wavelengths that significantly overlaps with the solar spectrum (Fig. 1b).

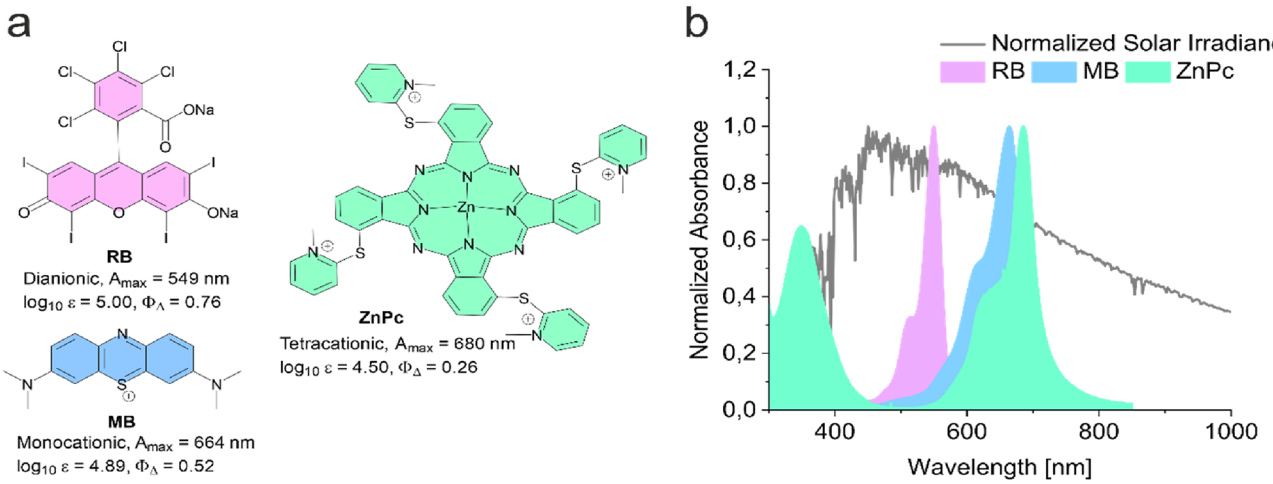

Fig. 1 (**a**) Structures and (**b**) UV–vis spectra of photosensitizers used in this study together with the solar irradiance spectrum

2 Materials and methods

2.1 General

All solvents, chemicals, buffer salts, and nutrient broth were purchased from Fisher Scientific, TCI, Sigma-Aldrich, Acros Organics, or Alfa Aesar and used as received. Ultrapure deionized water was provided by Thermo Scientific Barnstead GenPure UV/UF Systems. Digital images were recorded with a Keyence Microscope VHX7000.

2.2 Scanning electron microscopy measurements

SEM images were taken using an Apreo S LoVac, Thermo Fisher Scientific scanning electron microscope with resolution: 1 nm at 1 kV, 0.8 nm at 1 kV in immersion mode, 0.7 nm at 30 kV in STEM mode. To perform SEM measurements, the samples were sputter-coated with gold/palladium. ImageJ was used to determine the pore size of the materials [37]. The bulk density and open porosity were measured and calculated by Archimedes' principle according to the normed formula

$$\pi = \frac{M3 - M1}{M3 - M2} \times 100$$

where $M1$ is the mass of the sample as such, $M2$ the mass of the sample in ethanol, and $M3$ the mass of the sample after being soaked with ethanol and exposed again to the air.

2.3 Singlet oxygen detection

Photophysical measurements were done using a FluoroMax-Plus spectrophotometer from Horiba scientific. Materials were cut into ca. 3 × 3 × 3 mm cubes and washed with 70% ethanol solution (1 × 1 mL) and water (3 × 1 mL) to remove unbound PS. Then they were immersed into the cuvette also containing a magnetic stirrer (Fig. S3, Supporting Information). 3 mL 9,10-Anthracenediyl-bis(methylene)dimalonic acid (ABDA) solution in water was added. After irradiation with Xe-lamp containing a cut-off filter at 420 nm (30 mW/cm^2, spot size approx. 20 × 20 cm) for defined time (30 to 210 s) emission was measured. Measurements were done in duplicate.

2.4 Bacterial strains and culture conditions

B. subtilis strain DM 10 and *E. coli* strain Nissle 1917 were grown on lysogeny broth (LB) agar and kept at 4 °C. A single isolated colony was picked from this plate, transferred to 3 mL LB broth, and incubated aerobically overnight at 37 °C in a shaker incubator at 180 rpm (rotations per minute). The following day, bacteria were suspended in 10 mL of fresh LB medium to an optical density $OD_{600} = 0.1$ and grown in a flask to attenuation of approximately $OD_{600} = 0.5$. Thereafter, the bacterial suspensions were centrifuged at 4000 rpm for 5 min, re-suspended in a buffer solution to the final bacterial concentration of approximately 1×10^7 cells per mL and used in photo-inactivation experiments.

2.5 Photo-inactivation of bacteria

Before irradiation, the nanomaterials were treated with 70% aqueous ethanol solution overnight and then washed with a sufficient amount of phosphate buffered saline (PBS) to disinfect them and remove loosely bound PSs. For the batch experiments each ca. 3 × 3 × 3 mm cube was incubated with 500 µL bacterial suspension for 15 min and irradiated with a Xe-lamp containing a cut-off filter at 420 nm with irradiance 10 mW/cm^2 for 15 min (overall light dose 9 J/cm^2) and 30 min (overall light dose 18 J/cm^2). The HEIDOLPH Orbital Shaker was used to maintain a constant shaking speed of 300 rpm/min during irradiation, ensuring the sample was continuously agitated. For flow experiments the Flow Cell from BioSurface Technologies (FC 270) was used. Samples were punched to 12 mm diameter and 2 mm thickness probes to match the reactor size. Bacterial suspensions were pumped through the scaffold in a continuous flow at a speed of 5 rpm using a Matson Marlow peristaltic pump. At this time, the entire flow-through system is exposed to irradiation, and the collection of bacteria samples occurs after a specific period (which consists of multiple flow-through cycles) once they have emerged from the system. For all irradiation experiments a power meter (Solar Meter from Solartech) was used to measure light fluence rates regularly. After irradiation, viable bacterial cells were determined by serial dilutions of the bacterial suspension plated on Luria–Bertani agar plates and the number of colony forming units per ml (CFU/mL) was calculated after incubation at 37 °C overnight.

2.6 Statistical analysis

Data are expressed as mean ± standard deviation. Student's *t*-test and one-way analysis of variance within groups were used to compare the treatment effects. $p < 0.05$ was considered to represent a significant difference.

3 Results and discussion

3.1 Fabrication of scaffolds

For the fabrication of PDMS sponges we used the sugar cube template method [38]. PDMS is a thermally stable

compound, very flexible, hydrophobic and can be easily handled [39, 40]. It is a silicone based on organic polymers that has excellent elastomeric properties due to its chemical structure. Specifically, the chemical bonds between the silicon atom and the two oxygen atoms can be opened and closed, providing the molecule with a certain degree of flexibility [41]. To synthesize porous templates, generally sugar or salts are used, as they are well soluble in water. By using water, one can remove the templates easily, leaving the pores empty and ensuring flux throughout the sample.

For the fabrication of photoactive scaffolds Rose Bengal and Methylene Blue dissolved in ethanol at 1 mg/mL concentration were first poured onto commercial sugar cubes and put in a convection oven for about 30 min. To start with the PS at the comparable concentration, ssubstituted Zn(II) phthalocyanine was first dissolved in DMF at 10 mg/mL and diluted with ethanol to 1 mg/mL. Hence to remove all solvent a longer drying time was required for this sample: they were left in the oven for about 24 h. A 10:1 ratio mixture of PDMS prepolymer (Sylgard 184 A, Dow Corning) and curing agent (Sylgard 184 B, Dow Corning) was placed in a Petri dish and degassed in a vacuum chamber for 20 min to remove air bubbles. After that, the coloured sugar cubes were added to the PDMS precursor and then set under vacuum for an additional 3 h filling the empty pores of the sugar cube with PDMS precursor. The filled sugar cubes were then placed in a convection oven at 50 °C and cured for 3 h. After curing, the sugar was dissolved by slowly stirring in water, leaving behind a PDMS/photosensitizer sponge. The remaining water in the PDMS sponge was dried in the convection oven at 40 °C for 30 min (Fig. 2).

3.2 Characterization of materials

SEM images were recorded to estimate the average pore size and to look at the inner structure. The bulk density and open porosity were measured and calculated by Archimedes' principle.

Figure 3 shows the bulk density (black open circles) and the open porosity (red filled squares) measured for all the samples of this study. The values of the density range from 0.37 g/cm^3 for a sugar cube without PS to 0.39 g/cm^3 for sponges with ZnPc, giving an average value of 0.38 g/cm^3. The open porosity of all samples was on average 62%, a usual value for sponges like these with interconnected pores and long channels all along their structures [42], as confirmed by the SEM pictures. The sponges are very porous and permeable, this being of great help when they are used in water as filters, since they guarantee good continuous flow keeping their structure (almost) unaltered.

Typical SEM images of the PDMS/PSs sponges are shown in Fig. 4. The sponges reproduce the structure of the sugar cubes very well. For all samples investigated, macropores and interconnected 3D frameworks are observed. Due to the absence of other materials, such as particles or dopants, the pores are clearly visible and well defined, with an average

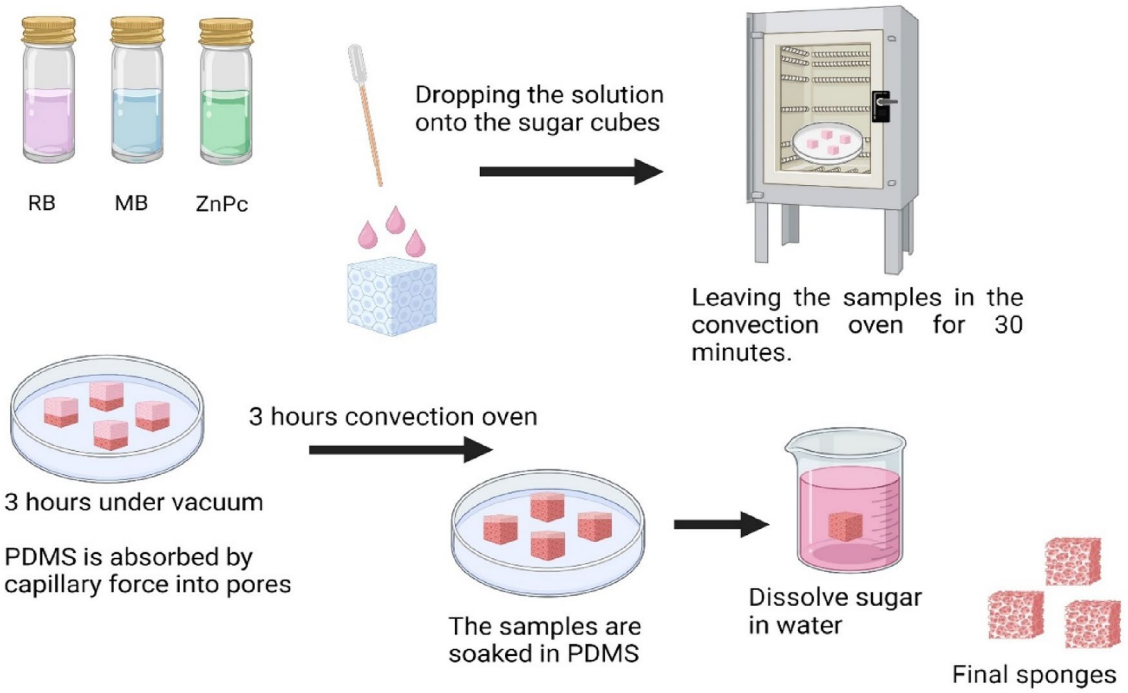

Fig. 2 Schematic illustration of the preparation of photoactive cubes using various photosensitizers and PDMS as carrier polymer

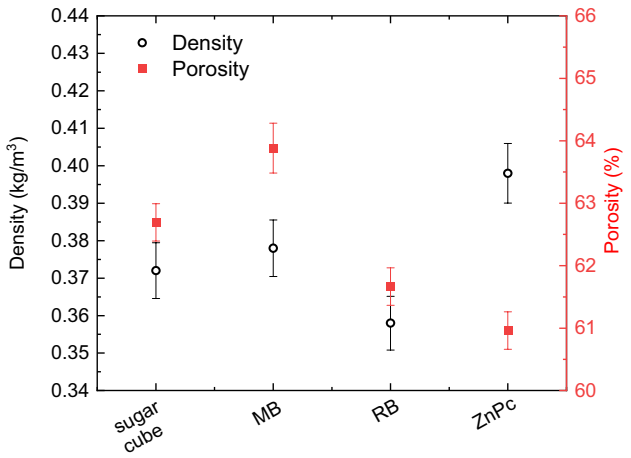

Fig. 3 Density (open black dots) and open porosity (red filled squares) of the PDMS/PSs sponges, determined via Archimedes' principle. For comparison, we also measured it on sponges without PS (also shown in figure)

size of about 110 micron (see Table 1). Pores are mostly spherical with smooth walls. Some crumples and protrusions can be seen on the edges of the pores, possibly caused by scratching during sugar removal. The presence of PSs does not alter the structure of the sponges themselves (See Fig. S1, supporting Information). In Table 1 we have summarized the values of the average pore size for each sponge/photosensitizer mixture.

Energy dispersive X-ray spectroscopy (EDS) was performed to detect the presence of selected elements in the sponges. In Fig. 5 the EDS mapping analysis of all investigated samples is shown. Silicon and carbon are present in every sample from the PDMS. Furthermore, we could detect chlorine in the sponges containing RB and zinc in the sponges containing ZnPc, which are rather homogeneously distributed over the sponges, confirming that the sugar template method works well for the preparation of these materials and that the PSs are not washed-out during sugar removal.

The 3D structure of the sponges was also examined using a digital microscopy (Keyence VHX 7000) (Fig. 6). The 3D images confirm our assumptions that the PSs have penetrated

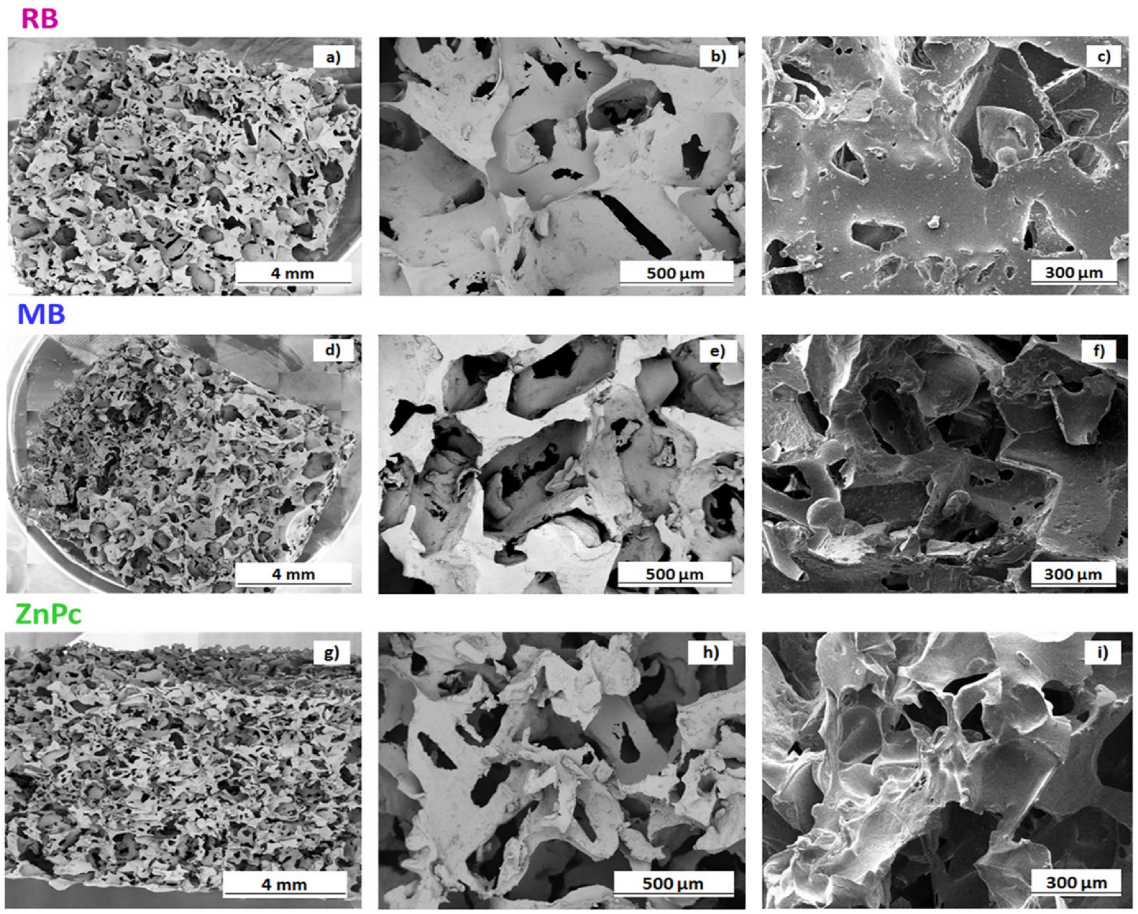

Fig. 4 SEM images of the investigated samples at different magnification scales. (**a**, **b**, **c**): Rose Bengal; (**d**, **e**, **f**): Methylene Blue; (**g**, **h**, **i**): ZnPc

Table 1 Average pore size of the three different samples according to the SEM images

Sample	Average pore size
RB	113 ± 3 µm
MB	117 ± 3 µm
ZnPc	116 ± 2 µm

throughout the cubes and did not remain on the surface only. This is beneficial in terms of photosensitization treatment, as all bacteria implanted can experience the effect of the treatment and be properly addressed, regardless of them being on the surface or inside the sponge. While the primary factor influencing the coloration of PS-loaded materials is typically the specific PS and its loading efficiency, it is worth noting that secondary interactions between PS molecules and the polymer carrier could potentially contribute to the coloration as well. Regarding MB, prior publications have noted that loading cellulosic derivatives with MB species imparts a blue hue. As the concentration of the PS increased, the MB-encapsulated polymer exhibited a purple coloration due to the aggregation of MB molecules facilitated by noncovalent π-π stacking interactions among their aromatic rings [43]. The blue color of the sample obtained in this study indicates the presence of monomeric and dimeric MB in the structure (Fig. S2, Supporting Information).

3.3 Generation of reactive oxygen species (ROS)

PDT is considered a versatile therapeutic approach due to its ability to target multiple metabolic pathways and cellular structures across a wide range of bacteria types, thanks to the action of photogenerated ROS. This makes PDT a comprehensive and effective mode of treatment, as opposed to focusing on a singular process or structure. When the photosensitizer is exposed to light of the right wavelength, it transfers its energy to molecular oxygen, resulting in the production of mainly singlet oxygen, however, generation of other types of ROS is not excluded. The validation of photosensitized generation of singlet oxygen ($^1O_2$) was done by immersing scaffolds in a solution with singlet oxygen-sensitive 9,10-Anthracenediyl-bis(methylene)dimalonic acid (ABDA) and exposing them to varying durations of irradiation, while stirring the solution (see Fig. S3, Supporting Information). The decrease in ABDA emission with increasing exposure time to light is illustrated in Fig. 7. This decrease occurs due to the formation of the non-fluorescent ABDA endoperoxide. Almost no changes in the spectra were observed when the scaffold did not contain any PS or when the samples were not irradiated. All PS-containing materials demonstrate the ability to sensitize the surrounding oxygen. The linear fit analysis reveals slight variations in the singlet oxygen generation rates, but these differences, which can be measured as the slopes of the linear fit, were not significant. Based on the results obtained, we propose that most likely mostly the PS on the scaffold surface effectively triggers the oxidation of ABDA, and hence despite the differences in $^1O_2$ generation of PS itself, the materials show comparable values of $^1O_2$ generation. Unfortunately, a reliable determination of the PS concentration in the samples after the washing steps was not possible due to the enormous stability and insolubility of the material in any solvent. Nevertheless, visual color inspection shows a higher concentration of ZnPc compared to MB and RB, which probably compensates for the lower yield of $^1O_2$ generation from PS in molecular form (0.26 for ZnPc, 0.76 for RB and 0.52 for MB).

3.4 Antibacterial performance of the materials

The materials were determined to be highly stable in both PBS, ethanol and complex media such as lysogeny broth (LB) and even in polar organic solvents such as DMF as no change of morphology was observed even after 10 weeks in the corresponding media. This renders them an ideal framework for water treatment applications. The study assessed the antibacterial effectiveness of the microporous samples against two typical generic bacteria the Gram-positive *B. subtilis* and the Gram-negative *E. coli*. Studies were performed by counting the number of colony-forming units (CFUs) on LB plates seeded with the bacterial suspension after being irradiated or kept in dark for a specified time in the presence of the corresponding material. The control groups (materials containing PS in the dark or material without PS) showed no bacterial inactivation under the same conditions—light dose or time, indicating that neither light nor the scaffold itself is lethal to bacteria.

Irradiation was performed in batch and in continuous flow systems as shown in Fig. 8a, b, as well as in Fig. S5 of Supporting Information. A consistent finding in all scaffolds containing PS was that extended exposure to light resulted in a higher degree of bacterial eradication. As can be seen from Fig. 8c B. *subtilis* demonstrate noticeable differences in viability upon irradiation. There was no bacterial damage observed in any of the control samples tested, while $>3\log_{10}$ reduction was observed after 15 min irradiation for all samples and $>5\log_{10}$ reduction after 30 min irradiation when RB was used as PS. Numerous studies have demonstrated that photosensitization can effectively deactivate Gram-positive bacteria using various dyes. However, Gram-negative bacteria possess a higher level of resistance and can only be eliminated using positively charged dyes or by enhancing the permeability of their outer membrane through chemical pre-treatment [44]. Under the same irradiation condition in batch none of the scaffolds showed any effect on *E.coli*. To ensure real-time functionality, we performed the irradiation experiments also in a continuous flow mode. While in batch mode samples were preincubated for 15 min, in

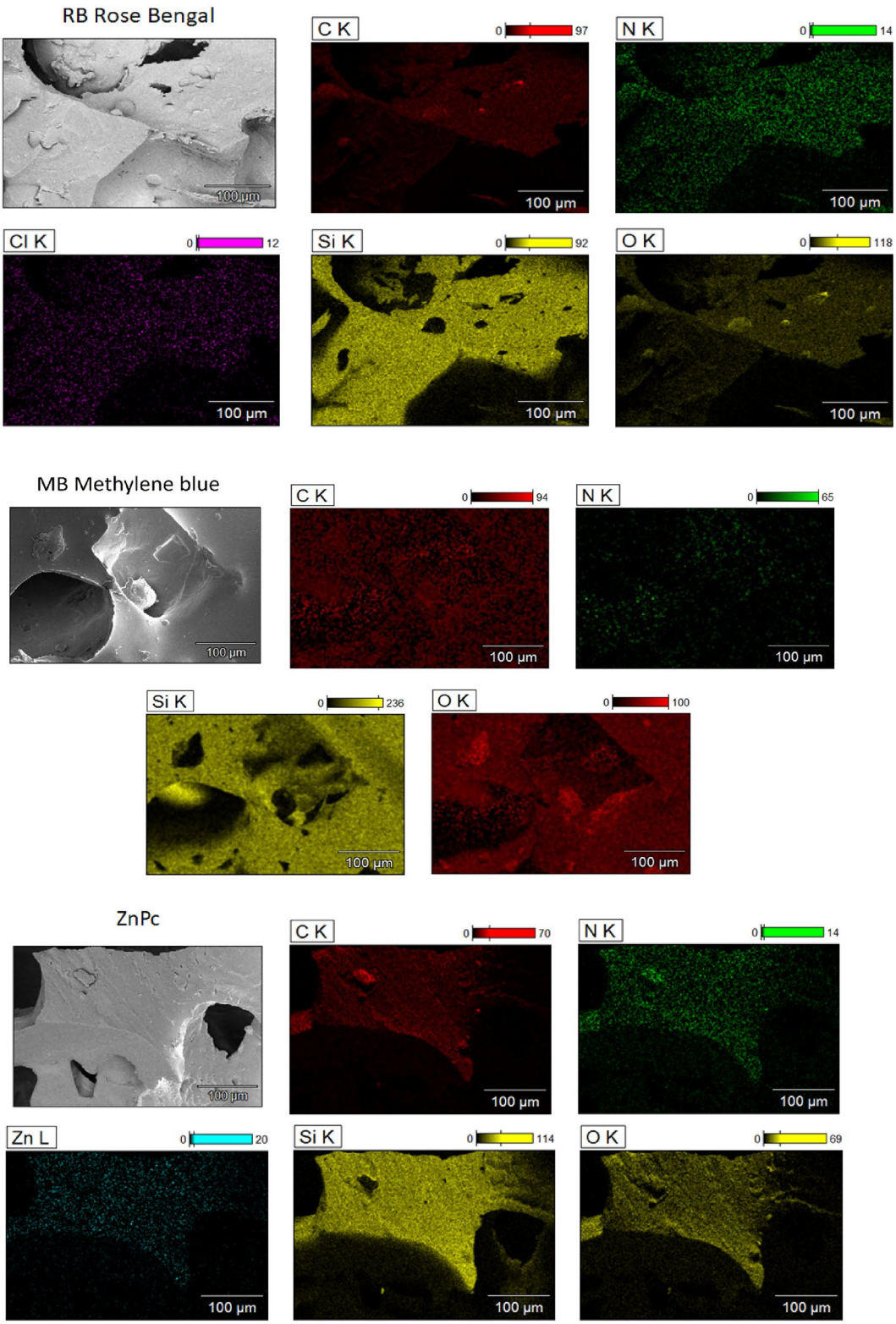

Fig. 5 EDS mapping analysis of all investigated samples

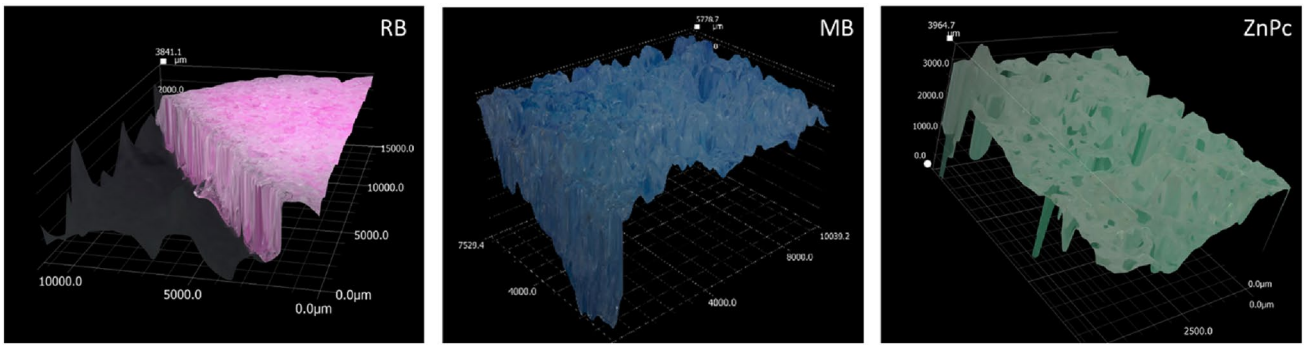

Fig. 6 Digital microscope images showing the 3D structure of the investigated sponges

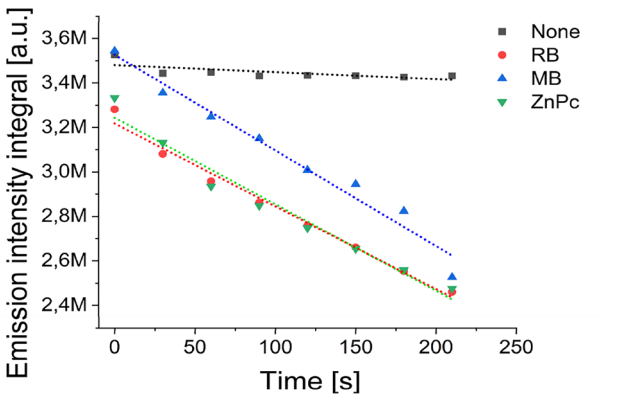

Fig. 7 First-order plots of ABDA degradation rate by microporous scaffolds in H_2O upon irradiation with a polychromatic light source with cut off filter at 420 nm

flow mode we first let the bacteria solution flow through for about 30 min before irradiation. Mechanical stress has a little effect (~ 1 $\log_{10}$ reduction) on *B. subtilis*, but no effect on the viability of *E.coli*. Two features need to be highlighted: as can be seen from Fig. 8d the inactivation rate constant for *B. subtilis* is much higher (up to 5 $\log_{10}$ reduction with all PS) in continuous flow mode than in batch. While in batch mode there is no effect on *E.coli* in flow experiment we could achieve 1.4 to 1.7 $\log_{10}$ reduction under the same irradiation conditions. These results confirm that (1) photodynamic damage is due to the diffusion of ROS, since we do not see very big difference between scaffold used and (2) as a result of flow increase inactivation occurs most likely due to the increase in bacteria-material interaction. This led us to conclude that overall chemical composition (PS and polymer) and architecture play the most important role for

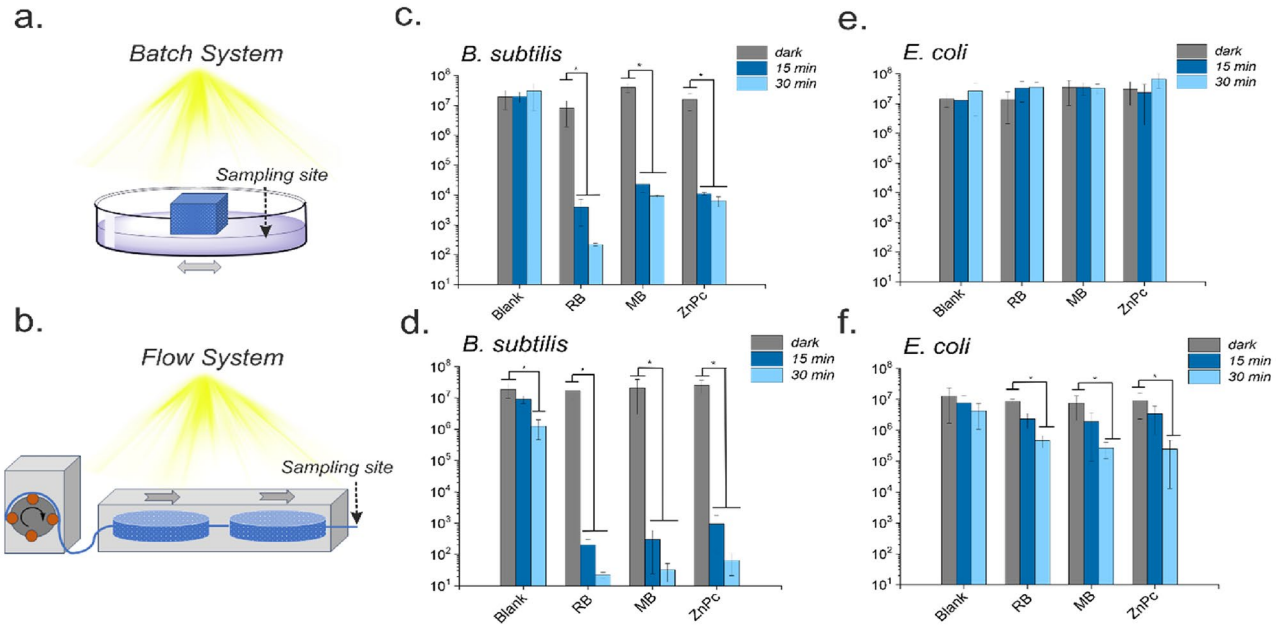

Fig. 8 Schematic illustration of batch (**a**) and flow (**b**) experimental systems. Histograms showing the reduction of bacteria viability upon irradiation (**c**–**f**). Irradiation conditions: polychromatic light with cut-off at 420 nm, irradiance 10 mW/cm^2

the construction of photoactive materials. A number of previous studies have shown that RB has great activity against Gram-positive bacteria when used as an antimicrobial PS but its activity against Gram-negative bacteria was found to be minimal, unless potassium iodide was used as adjuvant [45]. However, recent studies show that high concentrations of up to 6 $\log_{10}$ reduction of bacterial viability could be achieved when RB is used in a molecular form [46] or integrated in electrospun polyacrylonitrile nanofibers [47]. MB and ZnPc are positively charged, so efficacy against both bacterial strains was anticipated and known [36, 48]. Although leaching of PS per se could not be excluded, we assume that the light-triggered effectiveness comes from the materials themselves. Therefore, the adaptation and optimization of composition and structure plays just as an important role when manufacturing photoactive materials as the PS itself.

4 Conclusions

Killing microorganisms by visible light using photodynamic action is one of the most promising strategies for rapid and effective decontamination. (Nano)material-based approaches allow extension of the photodynamic action to many different fields, including water purification, due to the easy modulation of physicochemical properties and morphology of the material. In this study functional materials with light-assisted antimicrobial activity were fabricated using PDMS as carrier polymer and commercially available photosensitizers Rose Bengal and Methylene Blue and Zink(II) phthalocyanine derivative synthesized in our lab as PS. The obtained scaffolds are dimensionally stable, have micropore sizes, a large specific surface area and an excellent ability to diffuse through voids, which allowed for the development of a continuous flow system. Scaffolds were employed in both batch and continuous flow experiments for disinfection of water, using two common bacterial strains: Gram-positive *B. subtilis* and Gram-negative *E. coli*. The maximum photoinduced efficacy of ca. 5 $\log_{10}$ reduction of *B. subtilis* viability and ca. 2 $\log_{10}$ reduction of *E. coli* viability was achieved under flow condition.

Supplementary Information The online version contains supplementary material available at https://doi.org/10.1007/s43630-024-00544-3.

Acknowledgements We highly appreciate the financial support provided by the University of Duisburg-Essen, CENIDE and ZWU.

Funding Open Access funding enabled and organized by Projekt DEAL.

Data availability All data are available from the corresponding author upon request.

Declarations

Conflict of interest On behalf of all authors, the corresponding author states that there is no conflict of interest.

References

1. Murray, C. J. L., Ikuta, K. S., Sharara, F., Swetschinski, L., Aguilar, G. R., Gray, A., Han, C., Bisignano, C., Rao, P., Wool, E., Johnson, S. C., Browne, A. J., Chipeta, M. G., Fell, F., Hackett, S., Haines-Woodhouse, G., Kashef Hamadani, B. H., Kumaran, E. A. P., McManigal, B., … Mturi, N. (2022). Global burden of bacterial antimicrobial resistance in 2019: A systematic analysis. *Lancet, 399*, 629–655.
2. Jimenez, C. E. P., Keestra, S., Tandon, P., Cumming, O., Pickering, A. J., Moodley, A., & Chandler, C. I. R. (2023). Biosecurity and water, sanitation, and hygiene (WASH) interventions in animal agricultural settings for reducing infection burden, antibiotic use, and antibiotic resistance: A One Health systematic review. *Lancet Planet Health., 7*, e418–e434.
3. Hernando-Amado, S., Coque, T. M., Baquero, F., & Martínez, J. L. (2019). Defining and combating antibiotic resistance from One Health and Global Health perspectives. *Nature Microbiology, 4*, 1432–1442.
4. Nnadozie, C. F., & Odume, O. N. (2019). Freshwater environments as reservoirs of antibiotic resistant bacteria and their role in the dissemination of antibiotic resistance genes. *Environmental Pollution, 254*, 113067.
5. Zodrow, K. R., Li, Q., Buono, R. M., Chen, W., Daigger, G., Dueñas-Osorio, L., Elimelech, M., Huang, X., Jiang, G., Kim, J.-H., Logan, B. E., Sedlak, D. L., Westerhoff, P., & Alvarez, P. J. J. (2017). Advanced materials, technologies, and complex systems analyses: Emerging opportunities to enhance urban water security. *Environmental Science and Technology, 51*, 10274–10281.
6. Ma, B., Ke, Q., & Ulbricht, M. (2023). Simultaneous removal of natural organic matters and copper (II) with ultrafiltration for drinking water treatment. *Journal of Membrane Science, 671*, 121408.
7. Wang, Y., Ma, B., Ulbricht, M., Dong, Y., & Zhao, X. (2022). Progress in alumina ceramic membranes for water purification: Status and prospects. *Water Research, 226*, 119173.
8. Daigger, G. T. (2009). Evolving urban water and residuals management paradigms: Water reclamation and reuse, decentralization, and resource recovery. *Water Environment Research, 81*, 809–823.
9. Larsen, T. A., Hoffmann, S., Lüthi, C., Truffer, B., & Maurer, M. (2016). Emerging solutions to the water challenges of an urbanizing world. *Science, 352*, 928–933.
10. Priyadarshini, M., Das, I., Ghangrekar, M. M., & Blaney, L. (2022). Advanced oxidation processes: Performance,

advantages, and scale-up of emerging technologies. *Journal of Environmental Management, 316*, 115295.
11. Zhai, Q., Song, L., Ji, X., Yu, Y., Ye, J., Xu, W., & Hou, M. (2022). Research progress of advanced oxidation technology for the removal of Microcystis aeruginosa: A review. *Environmental Science and Pollution Research, 29*, 40449–40461.
12. Richards, B. S. & Schäfer, A. I. (2010). Chapter 12. Renewable energy powered water treatment systems. In I. C. Escobar, & A. I. Schäfer (Eds.), *Sustainability science and engineering* (pp. 353–373). Elsevier.
13. Rani, A., Snyder, S. W., Kim, H., Lei, Z., & Pan, S.-Y. (2022). Pathways to a net-zero-carbon water sector through energy-extracting wastewater technologies. *NPJ Clean Water, 5*, 49.
14. Hossain, F., Perales-Perez, O. J., Hwang, S., & Román, F. (2014). Antimicrobial nanomaterials as water disinfectant: Applications, limitations and future perspectives. *Science of the Total Environment, 466–467*, 1047–1059.
15. Li, Q., Mahendra, S., Lyon, D. Y., Brunet, L., Liga, M. V., Li, D., & Alvarez, P. J. (2008). Antimicrobial nanomaterials for water disinfection and microbial control: Potential applications and implications. *Water Research, 42*, 4591–4602.
16. Wainwright, M., Maisch, T., Nonell, S., Plaetzer, K., Almeida, A., Tegos, G. P., & Hamblin, M. R. (2017). Photoantimicrobials—are we afraid of the light? *The Lancet. Infectious Diseases, 17*, e49–e55.
17. Aroso, R. T., Schaberle, F. A., Arnaut, L. G., & Pereira, M. M. (2021). Photodynamic disinfection and its role in controlling infectious diseases. *Photochemical & Photobiological Sciences, 20*, 1497–1545.
18. Galstyan, A. (2021). Turning photons into drugs: Phthalocyanine-based photosensitizers as efficient photoantimicrobials. *Chemistry—A European Journal, 27*, 1903–1920.
19. Hu, X., Zhang, H., Wang, Y., Shiu, B.-C., Lin, J.-H., Zhang, S., Lou, C.-W., & Li, T.-T. (2022). Synergistic antibacterial strategy based on photodynamic therapy: Progress and perspectives. *Chemical Engineering Journal, 450*, 138129.
20. DeRosa, M. C., & Crutchley, R. J. (2002). Photosensitized singlet oxygen and its applications. *Coordination Chemistry Reviews, 233–234*, 351–371.
21. Mesquita, M. Q., Dias, C. J., Neves, M. G. P. M. S., Almeida, A., & Faustino, M. A. F. (2018). Revisiting current photoactive materials for antimicrobial photodynamic therapy. *Molecules, 23*, 2424.
22. Zarrintaj, P., Moghaddam, A. S., Manouchehri, S., Atoufi, Z., Amiri, A., Amirkhani, M. A., Nilforoushzadeh, M. A., Saeb, M. R., Hamblin, M. R., & Mozafari, M. (2017). Can regenerative medicine and nanotechnology combine to heal wounds? The search for the ideal wound dressing. *Nanomedicine, 12*, 2403–2422.
23. Riesco, R., Boyer, L., Blosse, S., Lefebvre, P. M., Assemat, P., Leichle, T., Accardo, A., & Malaquin, L. (2019). Water-in-PDMS emulsion templating of highly interconnected porous architectures for 3D cell culture. *ACS Applied Materials & Interfaces, 11*, 28631–28640.
24. Wang, W., Zhou, M., & Yuan, D. (2017). Carbon dioxide capture in amorphous porous organic polymers. *Journal of Materials Chemistry A., 5*, 1334–1347.
25. Liang, J., Wang, S., Yu, H., Zhao, X., Wang, H., Tong, Y., Tang, Q., & Liu, Y. (2020). Solution-processed PDMS/SWCNT porous electrodes with high mass loading: Toward high performance all-stretchable-component lithium ion batteries. *Sustainable Energy & Fuels., 4*, 2718–2726.
26. Khurana, B., Gierlich, P., Meindl, A., Gomes-da-Silva, L. C., & Senge, M. O. (2019). Hydrogels: Soft matters in photomedicine. *Photochemical & Photobiological Sciences, 18*, 2613–2656.
27. Dong, J., Ghiladi, R. A., Wang, Q., Cai, Y., & Wei, Q. (2018). Protoporphyrin-IX conjugated cellulose nanofibers that exhibit high antibacterial photodynamic inactivation efficacy. *Nanotechnology, 29*, 265601.
28. Stoll, K. R., Scholle, F., Zhu, J., Zhang, X., & Ghiladi, R. A. (2019). BODIPY-embedded electrospun materials in antimicrobial photodynamic inactivation. *Photochemical & Photobiological Sciences, 18*, 1923–1932.
29. Galstyan, A., & Strokov, K. (2022). Influence of photosensitizer concentration and polymer composition on photoinduced antimicrobial activity of PVA- and PVA-chitosan-based electrospun nanomaterials cross-linked with tailor-made silicon(IV) phthalocyanine. *Photochemical & Photobiological Sciences, 21*, 1387–1398.
30. Sambiagio, C., & Noël, T. (2020). Flow photochemistry: Shine Some Light on Those Tubes! *Trends in Chemistry., 2*, 92–106.
31. Buglioni, L., Raymenants, F., Slattery, A., Zondag, S. D. A., & Noël, T. (2022). Technological innovations in photochemistry for organic synthesis: Flow chemistry, high-throughput experimentation, scale-up, and photoelectrochemistry. *Chemical Reviews, 122*, 2752–2906.
32. Williams, J. D., & Kappe, C. O. (2020). Recent advances toward sustainable flow photochemistry. *Current Opinion in Green and Sustainable Chemistry, 25*, 100351.
33. Zhu, D., Handschuh-Wang, S., & Zhou, X. (2017). Recent progress in fabrication and application of polydimethylsiloxane sponges. *Journal of Materials Chemistry A., 5*, 16467–16497.
34. Dąbrowski, J. M., Pucelik, B., Regiel-Futyra, A., Brindell, M., Mazuryk, O., Kyzioł, A., Stochel, G., Macyk, W., & Arnaut, L. G. (2016). Engineering of relevant photodynamic processes through structural modifications of metallotetrapyrrolic photosensitizers. *Coordination Chemistry Reviews, 325*, 67–101.
35. Spagnul, C., Turner, L. C., & Boyle, R. W. (2015). Immobilized photosensitizers for antimicrobial applications. *Journal of Photochemistry and Photobiology B: Biology., 150*, 11–30.
36. Galstyan, A., Majiya, H., & Dobrindt, U. (2022). Regulation of photo triggered cytotoxicity in electrospun nanomaterials: Role of photosensitizer binding mode and polymer identity. *Nanoscale Advances, 4*, 200–210.
37. Schneider, C. A., Rasband, W. S., & Eliceiri, K. W. (2012). NIH Image to ImageJ: 25 years of image analysis. *Nature Methods, 9*, 671–675.
38. Lee, S. Y., Kang, D., Jeong, S., Do, H. T., & Kim, J. H. (2020). Photocatalytic degradation of Rhodamine B dye by TiO2 and gold nanoparticles supported on a floating porous polydimethylsiloxane sponge under ultraviolet and visible light irradiation. *ACS Omega, 5*, 4233–4241.
39. Xia, Y., & Whitesides, G. M. (1998). Soft lithography. *Angewandte Chemie International Edition, 37*, 550–575.
40. Park, Y.-B., Im, H., Im, M., & Choi, Y.-K. (2011). Self-cleaning effect of highly water-repellent microshell structures for solar cell applications. *Journal of Materials Chemistry A., 21*, 633–636.
41. Mark, J. E., & Curro, J. G. (1983). A non-Gaussian theory of rubberlike elasticity based on rotational isomeric state simulations of network chain configurations. I Polyethylene and polydimethylsiloxane short-chain unimodal networks. *Journal of Chemical Physics, 79*, 5705–5709.
42. Durmus, F. Ç., Maiorano, L. P., & Molina, J. M. (2022). Open-cell aluminum foams with bimodal pore size distributions for emerging thermal management applications. *International Journal of Heat and Mass Transfer, 191*, 122852.
43. Mills, A., Hawthorne, D., Burns, L., & Hazafy, D. (2017). Novel temperature-activated humidity-sensitive optical sensor. *Sensors and Actuators, B: Chemical, 240*, 1009–1015.
44. Galstyan, A., & Dobrindt, U. (2019). Determining and unravelling origins of reduced photoinactivation efficacy of bacteria in milk.

Journal of Photochemistry and Photobiology B: Biology., 197, 111554.

45. Wen, X., Zhang, X., Szewczyk, G., El-Hussein, A., Huang, Y.-Y., Sarna, T., & Hamblin, M. R. (2017). Potassium iodide potentiates antimicrobial photodynamic inactivation mediated by rose bengal in in vitro and in vivo studies. *Antimicrobial Agents and Chemotherapy., 61*(7), e00467. https://doi.org/10.1128/aac.00467-17
46. Kurosu, M., Mitachi, K., Pershing, E. V., Horowitz, B. D., Wachter, E. A., Lacey, J. W., Ji, Y., & Rodrigues, D. J. (2023). Antibacterial effect of rose bengal against colistin-resistant gram-negative bacteria. *Journal of Antibiotics., 76*, 416–424.
47. Dong, X., Mitchell, D. G., Garcia Cervantes, M. Y., Chitara, B., Yang, L., & Yan, F. (2022). Rose bengal-integrated electrospun polyacrylonitrile nanofibers for photodynamic inactivation of bacteria. *Environmental Science: Advances, 1*, 736–745.
48. Gollmer, A., Felgenträger, A., Bäumler, W., Maisch, T., & Späth, A. (2015). A novel set of symmetric methylene blue derivatives exhibits effective bacteria photokilling—a structure–response study. *Photochemical & Photobiological Sciences, 14*, 335–351.